Foroozan Zare and Árpád Veress*

Novel Closed-Form Equation for Critical Pressure and Optimum Pressure Ratio for Turbojet Engines

https://doi.org/10.1515/tjj-2019-0039
Received October 07, 2019; accepted October 23, 2019

Abstract: Advanced mathematical model has been developed for design and analysis of turbojet engines. It includes closed form algebraic equation for critical pressure and optimum pressure ratio at maximum thrust. The model and the algebraic equations consider efficiencies, pressure recovery rates meanwhile the gas parameters are the function of the fuel to air ratio and the temperature. РД-9Б and АЛ-21Ф3 engines are applied for demonstrating the capabilities of the calculation process. The unknown parameters as efficiencies, pressure recovery rates, power reduction rate of the auxiliary systems, bleed air ratio, air income ratio due to blade cooling and total temperature in the afterburner were identified by constrained optimization. The effect of i. T_{04}/T_{02} ratio for the thrust and TSFC in the function of compressor pressure ratio, ii. the real (viscous) flow conditions and iii. the temperature and fuel to air ratio on gas parameters were also investigated for verification and plausibility check.

Keywords: jet engine, thermodynamics, cycle analysis of real engine, critical pressure ratio, optimum compressor pressure ratio

PACS® (2010). 07.20.Pe, 89.40.Dd, 05.70.-a, 88.05.Xj

Introduction

In these days, there are many ongoing researches in the field of aeronautics [1, 2]. Regarding the power generation, the application of heat engines is widespread not only in the aerospace industry, but in the oil, gas and energy sector too. Significant amount of research has been carried out in analyzing and developing gas turbine systems [3–5] and system components [6, 7].

The gas turbines are currently the only available propulsion systems for high-powered commercial and military airplanes. Although their thermodynamic cycles do not have high core thermal efficiency (~ 28 to 38 %), the jet engines have substantial advantages in overall power, power density, compactness, streamlining, simplicity and low maintenance cost demands. These power units are also less sensitive to overloads and produce less vibration due to the well balanceable and rather axisymmetric rotational components. The gas turbines have high availability (80–99 %), reliability, which can exceed 99 % and low emissions (there is no lubricant in the combustion chamber and no soot during transient loads). They have fewer moving parts and lower sensitivities to fuel composition. Additionally, gas turbines do not need a liquid-based cooling system, although the maximum allowable temperature (~ 1500 °C) at the turbine inlet section is limited due to metallurgical reasons [8].

Beside the technical level of gas turbines today, there are many possible areas for potential improvements of their efficiency, power and emissions. Although the experiences and the know-how of the gas turbine manufacturers are increasing continuously, developing more accurate mathematical models for determining the most suitable thermo-dynamical parameters and completing optimizations can significantly contribute to decrease cost, time and capacity in the early phases of design and developments. These are proven by the scientific literature too; there are many research publications deal with thermodynamic-based simulation approaches.

Homaifar et al. [9] presented an application of genetic algorithms to the system optimization of turbofan engines. The goal was to optimize the thrust per unit mass flow rate and overall efficiency in the function of Mach number, compressor pressure ratio, fan pressure ratio and bypass ratio. Genetic algorithms were used in this article because they were able to quickly optimize the objective functions involving sub functions of multivariate. Although the model used here to represent a turbofan engine is a relatively simple one, the procedure would be exactly the same with a more elaborate model. Results of assorted runs fixed

***Corresponding author: Árpád Veress,** Department of Aeronautics, Naval Architecture and Railway Vehicles, Faculty of Transportation Engineering and Vehicle Engineering, Budapest University of Technology and Economics, Műegyetem rkp. 3, Budapest H-1111, Hungary, E-mail: averess@vrht.bme.hu
Foroozan Zare, Department of Aeronautics, Naval Architecture and Railway Vehicles, Faculty of Transportation Engineering and Vehicle Engineering, Budapest University of Technology and Economics, Műegyetem rkp. 3, Budapest H-1111, Hungary, E-mail: fzare@vrht.bme.hu

Published online November 30, 2019

with experimental and single parameter optimization results. Chocked condition was not considered, and the air and gas properties were constant or averaged at the given sections of the engine based on the used reference.

Guha [10] determined the optimum fan pressure ratio for separate-stream as well as mixed-stream bypass engines by both numerical and analytical ways. The optimum fan pressure ratio was shown to be predominantly a function of the specific thrust and a weak function of the bypass ratio. The gas properties were constant in the expression of optimum fan pressure ratio for separate-stream bypass engines at real flow condition.

Silva and his co-workers [11] presented an evolutionary approach called the StudGA which is an optimization design method. The purpose of their work was to optimize the performance of the gas turbine in terms of minimizing fuel consumption at nominal thrust output, maximize the thrust at the same fuel consumption and minimizing turbine blade temperature.

Mattingly [12] published a detailed theoretical review about the rocket and gas turbine propulsion. There is a description also in that literature how the thermo-dynamical cycles determine the mean characteristic of the jet engines. The author presented a closed-form equation for the optimum compressor pressure ratio at maximum specific thrust at ideal (inviscid) flow condition. The effects of temperature and fuel to air ratio were not considered in parameters describe the gas properties.

As the revised references used simplifications as excluding the effect of chocked flow condition at converging nozzle flow and gas properties with considering the local temperature and fuel to air ratio for example, it also confirms the need for developing physically advanced, more accurate mathematical models, calculations and optimizations.

Single spool turbojet engines are frequently used in commercial and military applications due to their low normalized range factor[1] and low emissions at relatively high flight speed. Two turbojets of this type, the РД-9Б and the АЛ-21Ф3 were thus used for testing and verifying the results of the presently developed mathematical model. The РД-9Б was the first engine, which includes a supersonic stage compressor. It is a single-spool axial flow turbojet engine with a nine-stage compressor and an afterburner. The engine has a bleed air dump control system depending on the compression ratio. Following the compressor, the air flows through can annular combustion chambers mounted in a single cover. The axial flow turbine has two stages with a hydraulically-regulated nozzle situated behind the afterburner chamber. The РД-9Б was designed as a light, powerful engine for fighter aircraft, and it was used in the MiG-19S, MiG-19P, MiG-19PM and Yak-25 aircraft. The АЛ-21Ф3 turbojet aircraft engine is used in the Sukhoi Su-17, Sukhoi Su-24 and Sukhoi T-10. It can equal the GE J-79 engine as one of the most powerful supersonic engines in service today.

Although the hereinafter introduced new equations and the thermodynamic calculation methodology are valid for single spool turbojet engines, they can also be applied for other types of jet engines and goal functions in case of consistently adapted theoretical derivations.

Optimum compressor total pressure ratio at maximum specific thrust

New equations have been introduced in the present chapter for determining the optimum pressure ratio pertaining at maximum specific thrust. The expressions apply the real (viscous) flow assumptions and the temperature and mass fraction dependencies of the relevant gas properties.

New closed-form equation to determine the optimum compressor total pressure ratio

The derivation of the optimum pressure ratio at specific thermodynamic condition including losses and variable gas properties was based on finding the extreme value of the specific thrust in the function of the compressor total pressure ratio. Hence, as the first step, the expression of the thrust was introduced in eq. (1) [13].

$$T = [\dot{m}_9 V_9 - \dot{m}_{air} V_0] + A_9(p_9 - p_0) \tag{1}$$

The mass flow rate at the exhaust nozzle was determined by eq. (2) [14].

$$\dot{m}_9 = \dot{m}_{air}[(1 - \delta_{tech})(1 + f_{cc} + f_A)(1 + \delta_{bc})] \tag{2}$$

Concerning the well fitted converging-diverging nozzle, if the pressure ratio of the nozzle is over the critical one the flow at the exit has ambient pressure, the flow is unchoked and the velocity is supersonic. Converging-diverging nozzle was considered (see Figure 1) with correctly expanded flow conditions ($p_9 = p_0$) because of the

1 The range factor in this context is the fuel and engine masses are divided by the thrust, which force is reduced by the drag force of the nacelle at given speed and range.

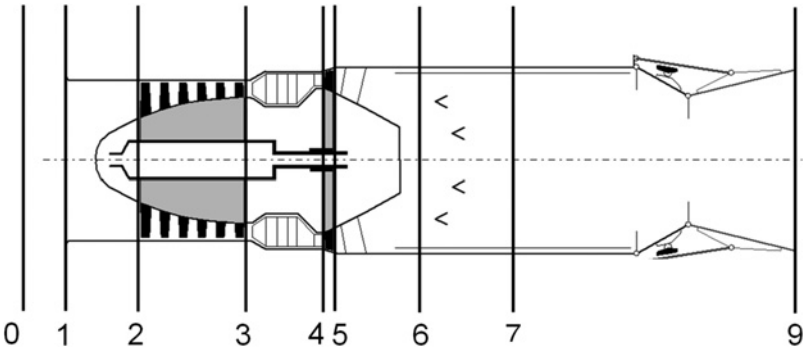

Figure 1: Layout of single spool turbojet engine with afterburner [15].

used engines. Furthermore, for extending the application range of the equation, the optimum compressor pressure ratio at maximum specific thrust was also derived for only converging nozzle at choked nozzle flow condition.

Unchoked flow condition at converging-diverging exhaust nozzle

As $p_9 = p_0$, only the outlet velocity (V_9) in eq. (1) depends on the compressor pressure ratio. Hence, the detailed derivation of the expression of the outlet velocity in the function of the compressor pressure ratio is introduced after introductory discussion about the gas properties.

Beside the unvarying gas properties such as specific gas constants, it is worth taking into consideration the effect of the local temperature and mass fraction when determining the specific heats at constant pressure and the ratios of the specific heats. These variables can be changed not only at each cross section of the engine, but also at different operational conditions in the function of the compressor pressure ratio. They can be determined as standalone or mean value depends on the application case. Iteration processes were applied in the followings if the temperature and/or mass fractions were the variables of the unknown parameters, to gain the equilibrium between the temperature dependent gas properties and the questionable unknown thermodynamic parameters [14].

In the derivation, first, the total enthalpy with the mean specific heat at constant pressure was expressed in eq. (3) to determine the total temperature at the outlet section of the engine.

$$h_{09} = h_9 + \frac{V_9^2}{2} \rightarrow \overline{C}_{pmix}(T_{09}, T_9, f)T_{09} = \overline{C}_{pmix}(T_{09}, T_9, f)T_9 + \frac{V_9^2}{2} \rightarrow T_{09} = T_9 + \frac{V_9^2}{2\overline{C}_{pmix}(T_{09}, T_9, f)} \tag{3}$$

Here, as usual, the fuel to air ratio, f was calculated by the available fuel mass flow rate divided by the available air mass flow rate at the investigated section.

The next step was to derive the velocity at the exit of the nozzle at thermodynamic condition with losses and variable gas properties in the function of the total pressure ratio of the exhaust nozzle (eq. (4)).

$$V_9 = \sqrt{2\overline{C}_{pmix}(T_{09}, T_{9s}, f)\eta_n T_{09}\left(1 - \frac{1}{(\pi_n)^{\alpha}}\right)} \tag{4}$$

Parameter α in eq. (4) is introduced in eq. (5). The goal of this simplification is to make the expression of the exhaust velocity more compact. The ratio of specific heats was calculated in the function of the temperature and fuel to air ratio according to eq. (6).

$$\alpha = \frac{\overline{\gamma}_{mix}(T_{07}, T_{9s}, f) - 1}{\overline{\gamma}_{mix}(T_{07}, T_{9s}, f)} \tag{5}$$

$$\overline{\gamma}_{mix} = \frac{\overline{C}_{pmix}(T_{09}, T_{9s}, f)}{\overline{C}_{pmix}(T_{09}, T_{9s}, f) - R_{mix}} \tag{6}$$

The total pressure ratio of the nozzle was expressed by the pressure ratio of the compressor and the turbine and the pressure recovery rate of the diffuser, combustion chamber and afterburner liner (see eq. (7)).

$$r_d\pi_C r_{cc} r_{al} = \pi_T \pi_n \Rightarrow \pi_n = \frac{r_d r_{cc} r_{al}\pi_C}{\pi_T} \tag{7}$$

By substituting eq. (7) into eq. (4) the velocity at the exhaust was reformulated as shown in eq. (8).

$$V_9 = \sqrt{2\overline{C}_{pmix}(T_{09}, T_{9s}, f)\eta_n T_{09}\left(1 - \left(\frac{\pi_T}{r_d r_{cc} r_{al} \pi_C}\right)^{\alpha}\right)} \tag{8}$$

The power balance of the compressor and turbine spool was used to establish the connection between the total pressure ratio of the compressor and the turbine (see eq. (9) and (10)) [16].

$$W_C = \eta_m W_T \tag{9}$$

$$\begin{aligned} &\dot{m}_2 \overline{C}_{pmix}(T_{02}, T_{03}, f = 0)(T_{03} - T_{02}) \\ &= \eta_m \dot{m}_4 (1 - \xi)\overline{C}_{pmix}(T_{04}, T_{05}, f_T)(T_{04} - T_{05}) \end{aligned} \tag{10}$$

$\dot{m}_2$ and $\dot{m}_4$ are the mass flow rates in the compressor and turbine respectively and are expressed in eq. (11).

$$\dot{m}_2 = \dot{m}_{air}, \quad \dot{m}_4 = \dot{m}_{air}[(1 - \delta_{tech})(1 + f_{cc})(1 + \delta_{bc})] \tag{11}$$

Eq. (12) was formed by replacing the mass flow rates in eq. (10) by eq. (11), introducing the isentropic efficiencies and isentropic relationship between the temperatures and pressures.

$$\begin{aligned} &\frac{1}{\eta_{C,s}}\overline{C}_{pmix}(T_{02}, T_{03}, f = 0)T_{02}\left((\pi_C)^{\beta} - 1\right) = \eta_m \eta_{T,s}(1 - \delta_{tech}) \\ &(1 + \delta_{bc})(1 + f_{cc})(1 - \xi)\overline{C}_{pmix}(T_{04}, T_{05}, f_T)T_{04}\left(1 - \frac{1}{(\pi_T)^{\varepsilon}}\right) \end{aligned} \tag{12}$$

β and ε in the superscripts represent compact forms of the exponents for the isentropic processes in the compressor and the turbine respectively (see eq. (13)). They are the function of the temperature and the local mass fraction of the air and burnt gases.

$$\beta = \frac{\overline{\gamma}_{mix}(T_{02}, T_{03s}, f = 0) - 1}{\overline{\gamma}_{mix}(T_{02}, T_{03s}, f = 0)}, \quad \varepsilon = \frac{\overline{\gamma}_{mix}(T_{04}, T_{05s}, f_T) - 1}{\overline{\gamma}_{mix}(T_{04}, T_{05s}, f_T)} \tag{13}$$

Parameter φ was introduced to include all the parameters in eq. (12) except for ε, π_T, π_c and β and it is shown in eq. (14).

$$\varphi = \frac{\overline{C}_{pmix}(T_{02}T_{03}, f = 0)}{\overline{C}_{pmix}(T_{04}T_{03}, f_{cc})}\frac{T_{02}}{T_{04}} \frac{1}{\eta_m \eta_{C,s}\eta_{T,s}(1 - \delta_{tech})(1 + \delta_{bc})(1 + f_{cc})(1 - \xi)} \tag{14}$$

Eq. (15) was formed by rearranging eq. (12) and for expressing the total pressure ratio of the turbine.

$$\pi_T = \left(1 - \varphi\left((\pi_C)^{\beta} - 1\right)\right)^{(-1/\varepsilon)} \tag{15}$$

The velocity at the exhaust of the nozzle (see eq. (16)) was derived by substituting eq. (15) into eq. (8).

$$V_9 = \sqrt{2\overline{C}_{pmix}(T_{09}, T_{9s}, f)\eta_n T_{09}\left[1 - \left(\frac{1}{\left(1 - \varphi\left((\pi_C)^{\beta} - 1\right)\right)^{\frac{1}{\varepsilon}}\pi_C \kappa}\right)^{\alpha}\right]} \tag{16}$$

κ in eq. (16) represents the multiplication of the pressure recovery rates in the diffuser, in the combustion chamber and in the afterburner liner ($\kappa = r_d r_{cc} r_{Al}$).

Finally, the specific thrust (eq. (17)) was expressed by inserting eq. (16) into eq. (1) at the start condition and at unchoked nozzle flow condition.

$$\frac{T}{\dot{m}_{air}} = [(1 - \delta_{tech})(1 + f_{cc} + f_a)(1 + \delta_{bc})] \sqrt{2\overline{C}_{pmix}(T_{09}, T_{9s}, f)\eta_n T_{09}\left[1 - \left(\frac{1}{\left(1 - \varphi\left((\pi_C)^{\beta} - 1\right)\right)^{\frac{1}{\varepsilon}}\pi_C \kappa}\right)^{\alpha}\right]} \tag{17}$$

The objective of the optimization process is to determine the optimum pressure ratio of the compressor, which pertains to maximum specific thrust. The reason of considering the specific thrust (thrust per unit mass flow rate of air) is to exclude the effect of compressor pressure ratio on the mass flow rate of air. The condition for the maximum specific thrust is shown by eq. (18) [14].

$$\frac{\partial\left(\frac{T}{\dot{m}_{air}}\right)}{\partial \pi_C} = 0 \tag{18}$$

Two sub steps of the derivation process are shown in the next two equations.

$$\frac{\partial\left(\frac{T}{\dot{m}_{air}}\right)}{\partial\pi_C} = -\frac{1}{2}\frac{[(1-\delta_{tech})(1+f_{cc}+f_a)(1+\delta_{bc})]\left[\frac{1}{\left(1-\varphi\left((\pi_C)^{\beta}-1\right)\right)^{\frac{1}{\varepsilon}}\pi_C}\right]^{\alpha}\cdot}{\cdot\alpha\left[\frac{\frac{\varphi(\pi_C)^{\beta}\beta}{\left(1-\varphi\left((\pi_C)^{\beta}-1\right)\right)^{\frac{1}{\varepsilon}}(\pi_C)^2\varepsilon\left(1-\varphi\left((\pi_C)^{\beta}-1\right)\right)}-\frac{1}{\left(1-\varphi\left((\pi_C)^{\beta}-1\right)\right)^{\frac{1}{\varepsilon}}(\pi_C)^2}}{\left(1-\varphi\left((\pi_C)^{\beta}-1\right)\right)^{\frac{1}{\varepsilon}}(\pi_C)}\right]}{\sqrt{1-\left[\frac{1}{\left(1-\varphi\left((\pi_C)^{\beta}-1\right)\right)^{\frac{1}{\varepsilon}}(\pi_C)}\right]^{\alpha}}} \tag{19}$$

$$\frac{\partial\left(\frac{T}{\dot{m}_{air}}\right)}{\partial\pi_C} = \frac{1}{2}\frac{[(1-\delta_{tech})(1+f_{cc}+f_a)(1+\delta_{bc})]\left[\frac{\left(1-\varphi(\pi_C)^{\beta}+\varphi\right)^{\frac{-1}{\varepsilon}}}{(\pi_C)}\right]^{\alpha}\alpha\left(\varphi(\pi_C)^{\beta}\beta-\varepsilon+\varepsilon\varphi(\pi_C)^{\beta}-\varepsilon\varphi\right)}{(\pi_C)\sqrt{1-\left[\frac{\left(1-\varphi(\pi_C)^{\beta}+\varphi\right)^{\frac{-1}{\varepsilon}}}{(\pi_C)}\right]^{\alpha}}\varepsilon\left(-1+\varphi(\pi_C)^{\beta}-\varphi\right)} \tag{20}$$

After completing the derivation and performing arrangements and simplifications, the final form of the optimum pressure ratio is shown in eq. (21).

$$\pi_{C\_opt} = \sqrt[\beta]{\frac{\varepsilon(1+\varphi)}{\varphi(\varepsilon+\beta)}} \tag{21}$$

Choked flow condition at converging exhaust nozzle

Although converging-diverging nozzle is used for such engines (РД-9Б and АЛ-21Ф3) as it is shown in Figure 1 the extension of the method is discussed in the present section for increasing the application range of the method for converging type nozzle at choked flow condition.

A similar procedure was applied to evaluate the optimum pressure ratio of the compressor in a choked condition as it was in the previous subchapter. The velocity at the exit of the converging nozzle is the speed of sound, when it is in a choked condition and it is not a function of the compressor pressure ratio explicitly. However, beside the exhaust velocity, the exhaust pressure (p_9 in eq. (1)) also contributes to generating thrust. This pressure is the critical pressure and can also be expressed in the function of the compressor pressure ratio as it is going to be shown below. The total pressures at the inlet and at the outlet section of the turbine were calculated by eq. (22) and (23) respectively.

$$p_{04} = r_{cc}\pi_C p_{02} \tag{22}$$

$$p_{05} = \frac{p_{04}}{\pi_T} = \frac{r_{cc}\pi_C p_{02}}{\left(1-\varphi\left((\pi_C)^{\beta}-1\right)\right)^{-\frac{1}{\varepsilon}}} \tag{23}$$

The total pressure at the inlet section of the nozzle (see eq. (24)) was determined by the turbine outlet total pressure and the total pressure recovery rate of the afterburner liner.

$$p_{07} = r_{Al}p_{05} = \frac{r_{cc}r_{Al}\pi_C p_{02}}{\left(1-\varphi\left((\pi_C)^{\beta}-1\right)\right)^{-\frac{1}{\varepsilon}}} \tag{24}$$

The total enthalpy and subsequently the total temperature at section "9" is introduced in the next steps (see eq. (25 and 26)).

$$h_{09} = h_9 + \frac{V_9^2}{2} \rightarrow \overline{C}_{pmix}(T_{09}, T_9, f)T_{09} = \overline{C}_{pmix}(T_{09}, T_9, f)T_9 + \frac{V_9^2}{2} \rightarrow T_{09} = T_9 + \frac{V_9^2}{2\overline{C}_{pmix}(T_{09}, T_9, f)} \tag{25}$$

$$T_{09} = T_9 + \frac{1}{\overline{C}_{pmix}(T_{09}, T_9, f)}\frac{V_9^2}{2}\frac{a_9^2}{a_9^2} \Rightarrow T_{09} = T_9 + \frac{1}{\overline{C}_{pmix}(T_{09}, T_9, f)}M_9^2\frac{\gamma_{mix}(T_9, f)RT_9}{2} \tag{26}$$

The critical condition corresponds to $M_9 = 1$ and $T_9 = T_c$, so the eq. (26) was reformulated accordingly. The isentropic static temperature at point "9" was expressed by the equation of isentropic nozzle efficiency and it is given by eq. (27).

$$T_{9s} = T_{09} - \frac{1}{\eta_n}\frac{(T_{09} - T_C)\overline{C}_{pmix}(T_{09,}\, T_C, f)}{\overline{C}_{pmix}(T_{09,}\, T_{9s}, f)} \tag{27}$$

The thermodynamic process between point 7 and 9s is isentropic (eq. (28)).

$$\frac{p_C}{p_{07}} = \left(\frac{T_{9s}}{T_{09}}\right)^{\frac{\overline{\gamma}_{mix}(T_{09}, T_{9s}, f)}{\overline{\gamma}_{mix}(T_{09}, T_{9s}, f)-1}} \tag{28}$$

A new closed-form expression (eq. (29)) was introduced to determine the critical pressure at the exit of the nozzle after substituting the isentropic static temperature in eq. (27) and the total temperature at nozzle exit in eq. (26) into eq. (28). Here, the dependencies of temperature variations and fuel to air ratios in the specific heats at constant pressure and so in the ratios of the specific heats were also considered. While the critical static pressure at the outlet section of the exhaust system was coupled with the total and static exit temperatures, iteration cycles were used to determine the corresponding critical pressure and all other thermodynamic parameters for the engine at choked condition. Eq. (29) gave higher critical pressure by 9.3 % for the РД-9Б engine than its original form with constant material data according to the theory of ideal gases (the ratio of specific heats for gas = 1.33 and for the air = 1.4).

$$p_9 = p_C = p_{07}\left[1 - \frac{1}{\eta_n}\left(1 - \frac{2\overline{C}_{pmix}(T_{09,}\, T_C, f)}{2\overline{C}_{pmix}(T_{09,}\, T_C, f) + \gamma_{mix}(T_C, f)R_{mix}}\right)\frac{\overline{C}_{pmix}T_{09,}\, T_C, f)}{2\overline{C}_{pmix}(T_{09,}\, T_C, f)}\right]^{\frac{\overline{\gamma}_{mix}(T_{09}, T_{9s}, f)}{\overline{\gamma}_{mix}(T_{09}, T_{9s}, f)-1}} \tag{29}$$

By substituting eq. (24) in eq. (29) and eq. (29) in eq. (1) the thrust can be expressed as follows:

$$T = [\dot{m}_9 V_9 - \dot{m}_{air} V_0] + A_9\left[\left(\begin{array}{c} p_{02}(r_{cc} r_{al}\pi_C)\left(1 - \varphi\left((\pi_C)^{\beta} - 1\right)\right)^{\frac{1}{\varepsilon}\cdot} \\ \cdot\left[1 - \frac{1}{\eta_n}\left(1 - \frac{2\overline{C}_{pmix}(T_{09,}\, T_C, f)}{2\overline{C}_{pmix}(T_{09,}\, T_C, f) + \gamma_{mix}(T_C, f)R_{mix}}\right)\frac{\overline{C}_{pmix}(T_{09,}\, T_C, f)}{2\overline{C}_{pmix}(T_{09,}\, T_C, f)}\right]^{\frac{\overline{\gamma}_{mix}(T_{09}, T_{9s}, f)}{\overline{\gamma}_{mix}(T_{09}, T_{9s}, f)-1}} \end{array}\right) - p_0\right] \tag{30}$$

The determination of the optimum pressure ratio pertaining at maximum thrust in choked converging nozzle flow conditions begins by completing the following derivation:

$$\frac{\partial T}{\partial \pi_C} = \left(\left(1 - \varphi(\pi_C)^{\beta} + \varphi\right)^{\frac{1}{\varepsilon}} - \frac{\left(1 - \varphi(\pi_C)^{\beta} + \varphi\right)^{\frac{1}{\varepsilon}}\varphi(\pi_C)^{\beta}\beta}{\varepsilon\left(1 - \varphi(\pi_C)^{\beta} + \varphi\right)}\right) \tag{31}$$

$$\frac{\partial T}{\partial \pi_C} = \left(\frac{\left(1 - \varphi(\pi_C)^{\beta} + \varphi\right)^{\frac{1}{\varepsilon}}\varepsilon - \left(1 - \varphi(\pi_C)^{\beta} + \varphi\right)^{-\frac{-1+\varepsilon}{\varepsilon}}\varphi(\pi_C)^{\beta}\beta}{\varepsilon}\right) \tag{32}$$

Completing the arrangements and simplifications, the final form of the expression for the optimum compressor total pressure ratio is given by eq. (33).

$$\pi_{C\_opt} = \sqrt[\beta]{\frac{\varepsilon(1+\varphi)}{\varphi(\varepsilon+\beta)}} \tag{33}$$

Based on eq. (21) and (33) the optimum pressure ratios for the convergent-divergent nozzle at correctly expanded flow condition ($p_9 = p_O$ and no shock waves form) and only convergent nozzle at choked condition are the same. This new closed-form explicit expression involves simplifications, because the gas properties and unknown variables – including efficiencies, pressure recovery rates and specific heats – and the incoming mass flow rate of air in case of choked converging nozzle were constant in the derivation process. Due to the proximity to the operational point, the presented approximation used the same recovery rates, efficiencies, power reduction rate of the auxiliary systems, bleed air ratio and air income ratio due to the blade cooling. Based on these simplification, further investigation is needed to determine its effect on the optimum total pressure ratio.

Mathematical model of the gas turbine

The description of the applied modeling approach and the results of the thermo-dynamical analysis of the gas turbines are discussed in the present chapter.

Introduction

A meridian cross section of a typical single spool turbojet engine with afterburner is shown in Figure 1. In the first section "0" represents the ambient conditions and "9" is the outlet of the exhaust nozzle. Real flow conditions were considered in the mathematical model of each segment of the assembly including pressure recovery factors and efficiencies as they were relevant. Temperature and fuel to air ratio dependencies were considered for specific heats as it is mentioned in the subchapter "Unchoked flow condition at converging-diverging exhaust nozzle".

Regarding the ambient conditions, static pressure and temperature at sea level were considered. These data were obtained from the ISA (International Standard Atmosphere): ambient static pressure: $p = p_0 = 101{,}325$ Pa, ambient static temperature: $T = T_0 = 288$ K, meanwhile the flight Mach number: $M = 0$. The reason of this start condition (maximum thrust at sea level) is that the engine specifications were available at that operational mode in the technical datasheet of the engines [17]. The extension of the below described method can be performed for high flight Mach number also in the next step of the present work.

The input parameters of the mathematical model can be divided into initially known and unknown parameters. The known input parameters were the incoming air mass flow rate, the pressure ratio of the compressor, the total temperature of the turbine inlet and the outlet cross section of the engine. The unknown parameters were the efficiencies (mechanical, isentropic of compressor and turbine, burning and exhaust nozzle), the pressure recovery rates (in the inlet diffuser, combustion chamber and afterburner or turbine exhaust pipe), the power reduction rate of the auxiliary systems, the bleed air ratio for technological reasons, the air income ratio due to blade cooling and the total temperature in the afterburner. Constrained optimization method was applied to determine the unknown parameters by recovering the thrust and thrust specific fuel consumption as the goal functions, which parameters were also available in the specification [17].

Analysis of single spool turbojet engines

РД-9Б and АЛ-21Ф3 turbojet engines at start condition (maximum thrust at sea level condition) have been considered for the analysis, for the verification of the simulation method and to test the new equations.

The related thermodynamic equations for each segment of the engine were already published in [18]. The calculation methodology summarized in the previous subchapter were used for the analysis. The known parameters of the engines are presented in Table 1. However, as noted before, there were also unknown parameters of the engines, which are shown in Table 2 and 3.

Table 1: Available operational data of the РД-9Б and АЛ-21Ф3 turbojet engines at start condition [17].

Type of turbojet engine	Known input data, which were used in the simulation			Known available data for parameter identification	
	T_{04} [K]	π_C	$\dot{m}_{air}$ [kg/s]	T[kN]	*TSFC* [kg/(kNh)]
Single spool engine (РД-9Б) with afterburner	1150	7.5	43.3	32.4	163
Single spool engine (АЛ-21Ф3) with afterburner	1385	15	104	110	190

Hence, an optimization method was used in a Matlab environment to determine these unknowns via parameter identification. The used function is called "Fmincon", and the approach is referred to as constrained nonlinear optimization or nonlinear programming, which applies a sequential quadratic programming (SQP) method [19]. In this case, the function solves a quadratic programming (QP) sub problem at each iteration. The method used trials with multiple restarts and repeated these until the maximum function evaluation limit is reached, or until the "Fmincon" algorithm would not significantly improve the current best solutions. The known thrust and thrust specific fuel consumption were the goal functions of the

Table 2: Identified parameters with the ranges of the investigated РД-9Б and АЛ-21Ф3 turbojet engines at start condition.

Type of turbojet engine	Pressure recovery rates and efficiencies of the engine components							
	r_d	r_{cc}	r_{Al}	$\eta_{C,s}$	$\eta_{T,s}$	η_m	η_b	η_n
Single spool turbojet engine with afterburner (РД-9Б)	0.9	0.94	0.91	0.83	0.87	0.995	0.97	0.95
Single spool turbojet engine with afterburner (АЛ-21Ф3)	0.9	0.93	0.89	0.82	0.88	0.99	0.94	0.92
Given ranges for the constrained optimization	0.88	0.93	0.88	0.81	0.87	0.99	0.94	0.92
	0.94	0.97	0.97	0.88	0.94	0.995	0.97	0.96

Table 3: Identified parameters and ranges of the investigated РД-9Б and АЛ-21Ф3 turbojet engines at start condition.

Type of turbojet engine	Power reduction rate of the auxiliary systems, bleed air ratio for technological reasons, air income ratio due to blade cooling and total temperature at the afterburner			
	ξ	δ_{tech}	δ_{bc}	T_{07}(K)
Single spool turbojet engine with afterburner (РД-9Б)	0.005	0.077	0.0534	1700
Single spool turbojet engine with afterburner (АЛ-21Ф3)	0.005	0.07	0.06	1900
Given ranges for the constrained optimization	0.005	0.02	0.05	1700
	0.01	0.18	0.06	2200

optimization, which were aimed to reach by modifying the unknown parameters over the given ranges. The results and range of each parameter (upper and lower limits) are found in Tables 2 and 3.

Table 4 shows that the resulted thrust and thrust specific fuel consumption of the optimization was close to the available data. The highest relative differences between the known and the resulted values in the parameter fitting is 0.0617 % for the thrust and 0.0245 % for *TSFC* at РД-9Б engine, while the unknown parameters are presented in Table 2 and 3 were within the expected intervals.

Table 4: The available and the resulted thrust and thrust specific fuel consumption used in the optimization for parameter identification.

Type of turbojet engine	Available data		Output of the optimization	
	T [kN]	*TSFC* [kg/(kN h)]	*T* [kN]	*TSFC* [kg/(kNh)]
Single spool turbojet engine (РД-9Б) with afterburner	32.4	163	32.42	162.96
Single spool turbojet engine (АЛ-21Ф3) with afterburner	110	190	110.	190

The thermodynamic cycle including real engine processes of the РД-9Б engine in the *T-s* diagram is plotted in Figure 2. The curves with smaller thickness represent the constant pressures. The processes between the engine states denoted by numbers were shown by thicker lines. This visualization effect is the reason for the constant pressure lines going below the process line in case of the pressure decrement just after sections “3” and “6”.

Numerical representation – verification of the new equations

The goal of the present chapter is to verify the correctness and investigate the accuracy of the new expression for the optimum compressor total pressure ratio. Hence, a numerical representation of the optimum pressure ratio was completed. In this context, the numerical representation is a searching algorithm over the expected pressure ratio range in order to find the total pressure ratio pertaining at maximum thrust. The same calculation method and the same parameters were used in the new expressions and in the numerical representation, which includes the application of the real (viscous) flow properties. The loss coefficients and other parameters which were previously unknown and were determined by the constrained optimization based on the available engine data, can change at different operational conditions and at different pressure ratios. However, in this work, these variations were not considered, and all these unknown parameters were assumed to be constant at all pressure ratios except for the isentropic compressor efficiency which is the function of the fixed polytrophic efficiency and compressor total pressure ratio for the fixed technology level. Figure 3

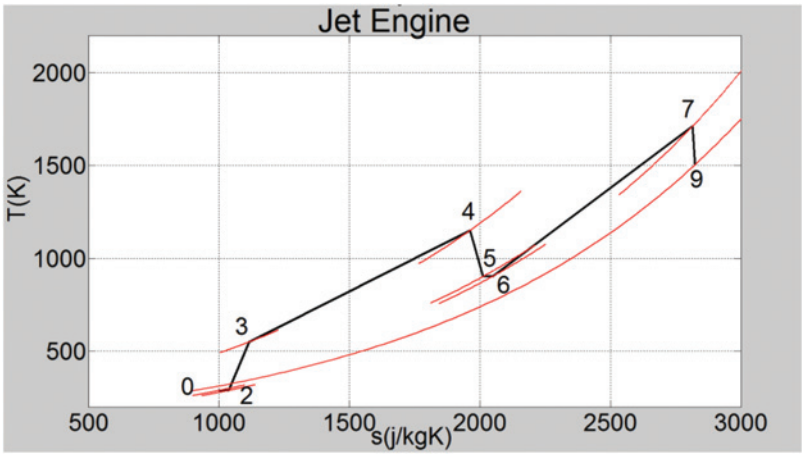

Figure 2: *T-s* diagram of the РД-9Б turbojet engine with afterburning.

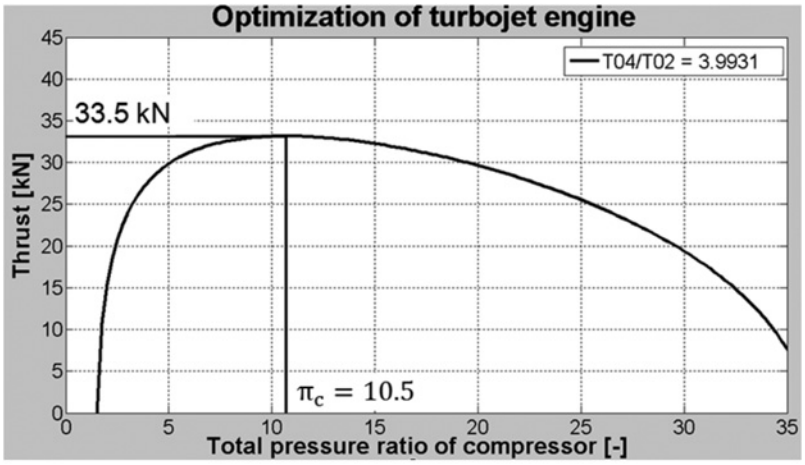

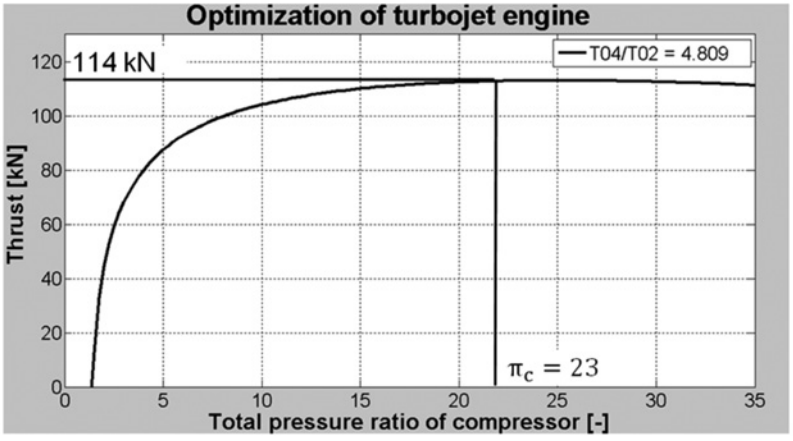

Figure 3: Thrust vs. total pressure ratio of the compressor for РД-9Б (top) and АЛ-21Ф3 (bottom) turbojet engines with afterburner.

shows the compressor pressure ratio-thrust function as numerical representation.

The optimum pressure ratios were 10.5 and 23 at maximum thrust 33,500 N and 114,000 N for РД-9Б and АЛ-21Ф3 respectively in the numerical representations. These values, provided by eq. (21 and 33), were 10.2 and 22.8, and the corresponding maximum thrusts were 33,680 N and 114,400 N respectively. The highest difference between the maximum thrusts using a numerical method and using the new equation

was 0.54 %. This deviation is due to the fact that the specific heats at constant pressure and parameters correspond to certain operational modes and the real flow assumptions in the specific thrust and thrust equations (eq. (17 and 30)) were assumed to be constant during the derivation. However, the resulting difference is negligible, and the results are accepted in engineering point of view.

The specific thrusts in the function of compressor total pressure ratios for the both engines are shown in case of correctly expanded converging-diverging nozzle flow conditions and at different T_{04}/T_{02} ratios in Figure 4. Higher turbine inlet temperature increases the specific thrust and the maximum values of that belong to higher compressor total pressure ratios.

The thrust specific fuel consumption in the function of compressor total pressure ratio for the both engines are shown in case of correctly expanded converging-diverging nozzle flow conditions and at different T_{04}/T_{02} ratios in Figure 5. The maximum specific thrust and minimum *TSFC* belong to the same compressor total pressure ratio ranges for the both investigated cases.

To determine the effect of the pressure recovery factors, efficiencies and parameter dependent specific heats for the thermodynamic cycle, for the optimum pressure ratio and so for the maximum thrust of a single spool turbojet engine, four different test scenarios were investigated. The results of this analysis are found in Table 5. The ■ sign in the column of viscous flow conditions means that the pressure recovery factors and efficiencies were considered in the calculation, meanwhile □ represents that they did not.

In case of the real flow conditions and variable specific heats, which were considered in the eq. (21 and 33), the optimum pressure ratio at the new equation was higher with 40 % and 53.3 % then the pressure ratio given in [17]. It corresponds to 3.39 % and 3.63 % thrust rising for РД-9Б and АЛ-21Ф3 jet engines respectively. In addition, besides keeping the viscous flow assumption, if the specific heat was defined to be constant, there was 9.52 % and 13.04 % decrement in the total pressure ratio for РД-9Б and АЛ-21Ф3 jet engines respectively. The non-real flow conditions – as inviscid and irrotational assumptions – provided unrealistic results; the thrust becomes double in comparing that

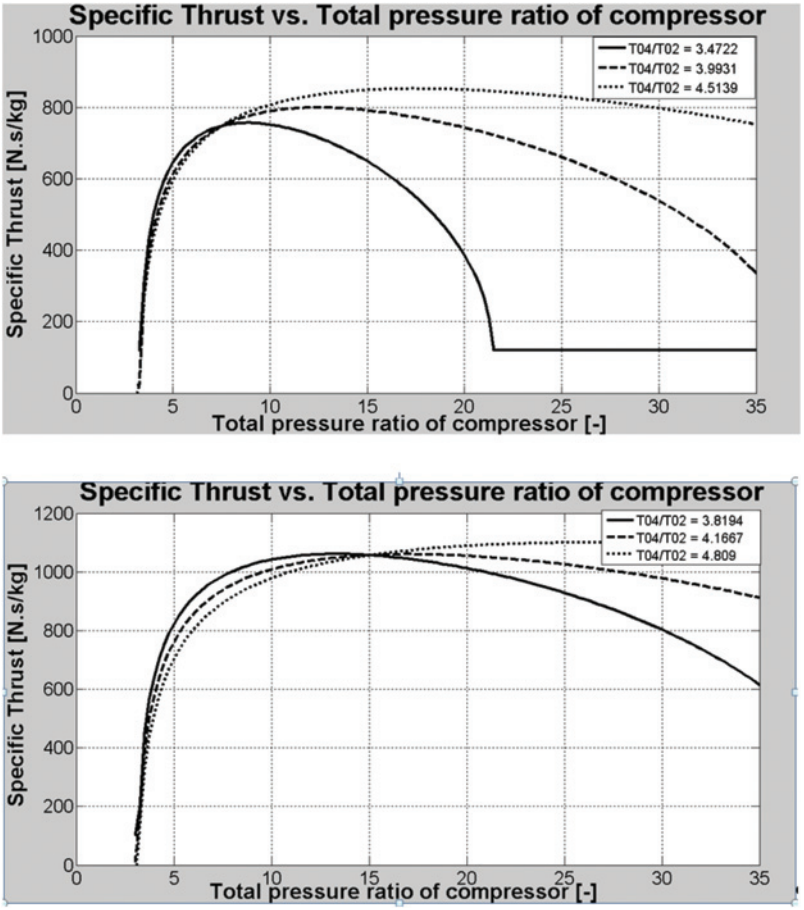

Figure 4: Specific thrust vs. total pressure ratio of the compressor for РД-9Б (above) and АЛ-21Ф3 (below) turbojet engines with afterburner.

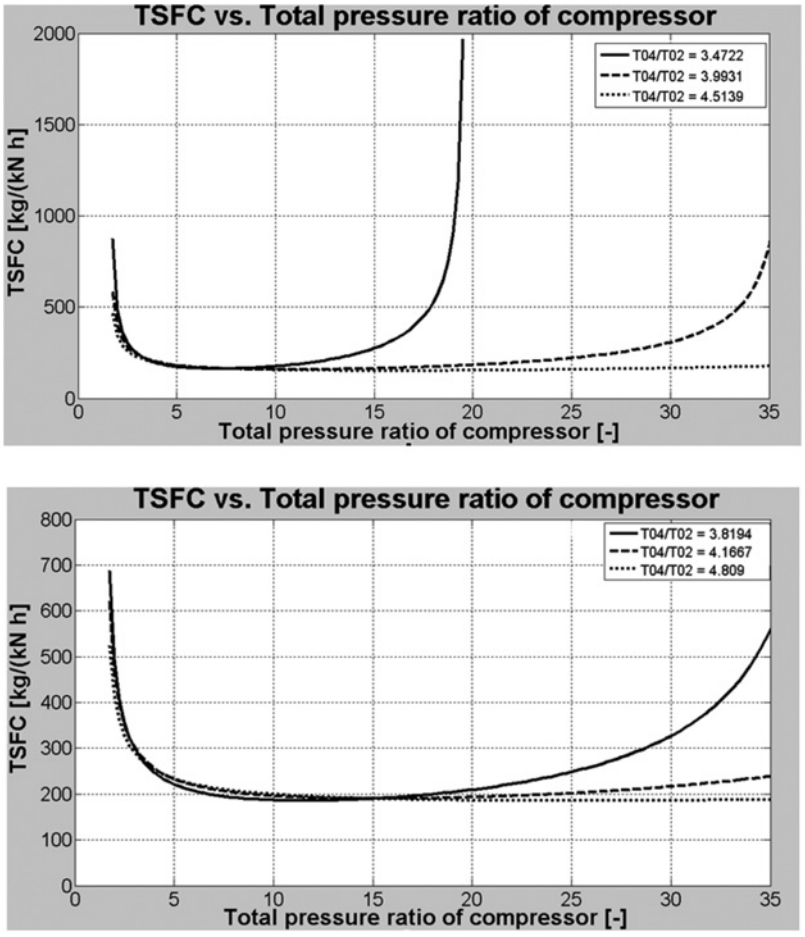

Figure 5: *TSFC* vs. total pressure ratio of compressor for РД-9Б (above) and АЛ-21Ф3 (below) turbojet engines with afterburner.

Table 5: The effect of gas properties (with and without temperature and fuel to air ratio dependencies) and real flow conditions (pressure recovery factors and efficiencies) for the optimal pressure ratio and thrust for the РД-9Б and АЛ-21Ф3 single spool turbojet engines.

	Viscous flow conditions	Gas properties	Optimum π_C by eq. (25 and 37)		Corresponding Max. Thrust [kN]	
			РД-9Б engine	АЛ-21Ф3 engine	РД-9Б engine	АЛ-21Ф3 engine
Present optimization study	☐	Dependent function by the fuel to air ratio of gas mixture and temperature	29	52	69.3	242.1
	☐	Constant	27	47	66.4	220
	■	Dependent function by the fuel to air ratio of gas mixture and temperature	10.5	23	33.5	114
	■	Constant	9.5	20	32.9	111.3

with the plausible approach. The best and the most realistic test scenario for having the maximum thrust was given by case that pressure recovery rates and efficiencies were considered, and the specific heats were assumed to be dependent functions of temperatures and fuel to air ratios.

The condition presented in eq. (18) is not sufficient to guarantee that the identified point is of the maximum thrust. The second derivative should also be checked. However, by having the similar result of the analytical method and numerical representation, it is not necessary to investigate the second derivative.

Conclusions

Today, the turbojet engines are the most relevant propulsion systems for aeronautical applications at low-speed supersonic flow regime between the low by-pass and ramjet engines and they can be considered to be an essential platform amongst the gas turbine engines in respect to establishing novel mathematical models. Design, development and analysis of such engines can be improved and accelerated by deriving new, simple and closed-form expressions with high accuracy for determining optimum operational conditions. Hence, an advanced thermo-dynamical model was developed for single spool turbojet engines – considering РД-9Б and АЛ-21Ф3 types in the analysis – which includes

i. a new closed-form expression to determine the critical pressure and
ii. a new equation for determining the optimum compressor total pressure ratio at maximum thrust.

These two equations mentioned in i. and ii. are valid at realistic thermodynamic (viscous flow) conditions via efficiencies and pressure recovery factors and at material and temperature dependent specific heats.

iii. The expression for critical pressure in case of choked flow in converging nozzle at viscous flow condition provided higher pressure by 9.3 % than the original equation (without considering efficiencies and pressure recovery factors and at constant gas properties).
iv. The plausibility of the new equation for the optimum total pressure ratio was verified by determining the extreme value of the pressure ratio-thrust functions numerically. The new equation for the optimum pressure ratio provides 3.39 % and 3.63 % thrust increment for the РД-9Б and АЛ-21Ф3 jet engines.
v. The presented modeling process and the new equations provide not only more accurate results for physical and technical processes but decrease the time for design, development and analysis of turbojet jet engines beside providing common platform for extending them for other type of engines too.

Nomenclature

Variables (Latin)	
A	Area, m^2
C_p	Specific heat at const. pressure, J/kg/K
$\bar{C}_p$	Mean spec. heat at const. pressure, J/kg/K
f	Fuel to air mass flow rates ratio, -
h	Specific Enthalpy, J/kg
$\dot{m}$	Mass flow rate, kg/s
M	Mach number, -
p	Pressure, Pa
r	Pressure recovery factor, -
R	Specific gas constant, J/kg/K
s	Specific entropy, J/kg/K
T	Temperature, K, Thrust, N
$TSFC$	Thrust Specific Fuel Consumption, kg/ (kNh)
V	Velocity, m/s
W	Power, W
Variables (Greek)	
γ	Ratio of specific heats, -
$\bar{\gamma}$	Ratio of mean specific heats, -
δ_{bc}	Air income ratio due to turbine blade cooling, -
δ_{tech}	Bleed air ratio for technological reasons, -
ξ	Power reduction rate of the auxiliary systems, -
η	Efficiency, -
π	Total pressure ratio,
Subscripts not referred above	
0x	Total
0-9	Engine cross sections
a	Afterburner
al	Afterburner liner
air	intake air
C	Compressor, Critical
cc	Combustion chamber
b	Burning
d	Diffuser
m	Mechanical
mix	Mass averaged of gas mixture
n	Nozzle
opt	Optimal
s	Isentropic
T	Turbine

Acknowledgements: This work was supported by Hungarian national EFOP-3.6.1-16-2016-00014 project titled by „Investigation and development of the disruptive technologies for e-mobility and their integration into the engineering education".

References

1. Rohacs D, Voskuijl M, Rohacs J, Schoustra RJ. Preliminary evaluation of the environmental impact related to aircraft take-off and landings supported with ground based (MAGLEV) power. J Aerosp Oper. 2014;2:161–80. DOI:10.3233/AOP-140040.
2. Bera J, Pokorádi L. Monte-Carlo simulation of helicopter noise. Acta Polytechnica Hungarica. 2015;12:21–32. DOI:10.12700/APH.12.2.2015.2.2.
3. Mclntire WL. A new generation T56 turboprop engine. Int J Turbo Jet Engines. 1985;2:189–98. DOI:10.1515/TJJ.1985.2.3.189.

4. Dimitrakopoulos P. A generalized method for the comparable and rigorous calculation of the polytropic efficiencies of turbocompressors. Int J Turbo Jet Engines. 2016;35:35–47. DOI:10.1515/tjj-2016-0029.
5. Dinc A. Optimization of a turboprop UAV for maximum loiter and specific power using genetic algorithm. Int J Turbo Jet Engines. 2015;33:265–73. DOI:10.1515/tjj-2015-0030.
6. Beneda K. Preliminary results of active centrifugal compressor surge control using variable inducer shroud bleed. Periodica Polytech Transp Eng. 2011;39:49–54. DOI:10.3311/pp.tr.2011-2.01.
7. Beneda K. Development of a modular FADEC for small scale turbojet engine, SAMI 2016 - IEEE 14th International Symposium on Applied Machine Intelligence and Informatics - Proceedings, art. no. 7422981, 2016:51–6. DOI:10.1109/SAMI.2016.7422981.
8. Beneda K, Simongáti G, Veress A. Járművek hő- és áramlástechnikai berendezései I. (Fluid- and turbomachinery in vehicles I (lecture note at BME)), ISBN 978-963-279-639-0, 1st ed., Budapest, Publisher: "Typotex Kiadó", Chapter 3,2012:73–5.
9. Homaifar A, Lai YH, McCormick E. System optimization of turbofan engines using genetic algorithms. Appl Math Modell. 1994;18:72–83. DOI:10.1016/0307-904X(94)90162-7.
10. Guha A. Optimum fan pressure ratio for bypass engines with separate or mixed exhaust streams. J Propul Power. 2001;17:1117–22. DOI:10.2514/2.5852.
11. Silva VV, Khatib W, Fleming PJ. Performance optimization of gas turbine engine. Artif Intell. 2005;18:575–83. DOI:10.1016/j.engappai.2005.01.001.
12. Mattingly JD, Boyer KM. Elements of propulsion: gas turbines and rockets, AIAA Education Series, Published by American Institute of Aeronautics and Astronautics, ISBN: 978-1-62410-371-1, 2006. DOI:10.2514/4.103711.
13. El-Sayed AF. Aircraft propulsion and gas turbine engines. Taylor & Francis Group, 2017. LLC, ISBN-13: 978-1-4665-9516-3 (Hardback).
14. Santa I. Repülőgép Hajtóművek (Aircraft Engines) I. (Gázturbinás Hajtóművek (Engines with Gas Turbines)), BME (Budapest University of Technology and Economics), Vasúti Járművek, Repülőgépek és Hajók Tanszék (Department of Aeronautics, Naval Architecture and Railway Vehicles), Tanszéki jegyzet (lecture note), Budapest, 2008.
15. Kurzke J. 2016, The gasturb program - commercial computer program, GasTurb12, [Online]. Available at: http://www.gasturb.de. Accessed: 30 Sep 2017.
16. Lugo-Leyte R, Salazar-Pereyra M, Lugo Méndez HD, Aguilar-Adaya I, Ambriz-García JJ, Vázquez Vargas JG. Parametric analysis of a two-shaft aeroderivate gas turbine of 11.86 MW. Entropy. 2015;17:5829–47. DOI:10.3390/e17085829.
17. КУЛАГИН ВВ, others. Теория расчёт и проектирование авиационных двигателей и энергетических установок. Moscow, 2005:438. ISBN: 5-217-03269-3.
18. Zare F, Veress A. Development and verification of an improved thermo-dynamical model for single spool jet engines. Repüléstudományi Közlemények (Publications in Aeronautical sciences) On-line Sci J. 2014;XXVI:539–51.
19. Mathworks, Matlab R2017b Documentation (Optimization Toolbox; "fmincon" function). 2017. [Online]. Available at: https://uk.mathworks.com/help/optim/ug/fmincon.html. Accessed: 30 Sep 2017.